Novel high-durability luminescent solar concentrators based on fluoropolymer coatings

Gianmarco Griffini*, Marinella Levi, Stefano Turri

Department of Chemistry, Materials and Chemical Engineering "Giulio Natta", Politecnico di Milano, Piazza Leonardo da Vinci 32, 20133 Milano, Italy

Received 10 September 2013
Received in revised form
13 November 2013
Accepted 16 November 2013
Available online 8 December 2013

1. Introduction

In the field of sunlight conversion and management, polymer-based luminescent solar concentrators (LSCs) have recently gained increasing attention as they represent a promising technology to reduce manufacturing and installation costs of traditional photovoltaic (PV) systems and simultaneously overcome some of the limitations presented by standard silicon-based PV devices, namely their heavy weight, poor response under diffuse sunlight and limited choice of colors and shapes [1]. In its most basic layout, the LSC consists of a transparent polymeric host matrix in which one or more luminescent species are embedded. The incident sunlight is absorbed by the luminescent molecules and is then re-emitted at a longer wavelength. Being the refractive index of the host matrix higher than that of air, a fraction of the re-emitted light is trapped within the polymer by total internal reflection, becoming concentrated along the edges of the plate, where it can be collected by small area solar cells [2]. By matching the emission spectrum of the luminophore to the band gap of the PV cell, PV device operation can be optimized and the price-per-watt of solar electricity can be significantly reduced [3–5]. Moreover, because of its light weight, color and shape tunability and ability to work well under diffuse light, LSC technology is particularly attractive for building-integrated PV applications and for installation in urban areas, where it could offer interesting possibilities to architects and building designers [6–8].

Two typical device configurations are commonly used in LSC technology, namely the bulk-plate and the thin-film LSC. In the first and more conventional case, a polymeric slab that also serves as the waveguide is homogeneously and lightly doped with the luminescent species. In the second case, a thin polymeric film more heavily doped with the luminescent species is deposited onto a transparent substrate, such as glass. Although no significant differences in performance can be found between these two configurations, thin-film LSCs present some technological advantages compared to conventional bulk-plate LSCs, as they can be easily deposited as thin luminescent coatings on a wide range of substrates by means of deposition techniques typical of the coating industry [9].

Intense research efforts have been made in past few years to achieve optical concentrations and device efficiencies suitable for practical applications. In particular, a variety of new luminescent species with high efficiency and improved photostability have been

* Corresponding author. Tel.: +39 02 2399 3213.
E-mail address: gianmarco.griffini@polimi.it (G. Griffini).

developed for use in LSC including organic dyes, inorganic phosphors and quantum dots [10–14]. Despite the encouraging results obtained with these high performing luminescent materials in terms of device efficiency, LSC commercial deployment is still hampered by the limited lifetime of the operating devices. In addition to the degradation of the luminescent species (organic dyes in particular) [15,16], the poor stability of the polymeric host matrix when subjected to continuous illumination still represents an obstacle to achieve prolonged LSC device lifetime. Nowadays, poly(methyl methacrylate) (PMMA) represents the material-of-choice for the polymeric host matrix in standard LSC devices because of its high transparency, its high refractive index and its easy processability [17]. However, its limited photostability as thin coating [18–20] can severely impact on the lifetime of PMMA-based LSC devices. In fact, degradation of the polymeric coating may lead to the formation of photon trapping sites that may decrease the photon transport efficiency [21,22]. In addition, radical species forming during polymer photodegradation may interact with the luminescent organic dye molecule resulting in degradation and decreased fluorescence quantum yield of the luminophore [23]. Recently, a great deal of attention has been devoted to the development of new LSC host matrix systems alternative to PMMA [24–27] that have led to improvements in LSC device optical efficiency. However, none of these materials has proven to be a promising candidate to achieve improved LSC device lifetime compared to PMMA under prolonged light exposure. Therefore, alternative polymeric systems that can ensure significantly improved outdoor stability of LSCs are still needed.

In a recent work by our group [28], it was demonstrated that some fluorinated polymers crosslinked with aliphatic polyisocyanate may represent an interesting alternative to PMMA to fabricate higher durability thin-film LSC devices. In fact, fluorinated polymers represent a class of high-performance materials that rely on the superior strength of the carbon-fluorine bond to achieve outstanding durability, weatherability and chemical resistance [29,30]. It is well known that consolidated industrial uses of fluorinated polymers span from the coil coating field to the heavy duty and water/oil repellency [31,32]. In addition, their use in the field of energy storage and conversion has also been recently demonstrated [33–35]. The innovative use of fluoropolymeric coatings in the LSC technology may open up new possibilities for the design and fabrication of LSC devices with excellent long-term durability. In order to achieve that, a thorough understanding of the relationship between the modifications occurring to these materials upon light exposure and the PV behavior of the corresponding LSC devices is however necessary and still to be accomplished.

In the present work, a detailed characterization of fluorescent fluorinated coatings upon long term light exposure (over 1000 h of UV–vis light irradiation) is presented in the attempt to correlate LSC device efficiency with chemical, physical and morphological modifications occurring to the fluorescent coating upon light exposure. In order to evaluate the influence of the type of crosslinking network on the durability of the coating, different crosslinking agents are employed, yielding different crosslinking chemical functionalities. It is shown that superior long-term operational stability compared to reference PMMA-based devices can be obtained with the new fluorinated coatings by appropriate selection of crosslinking agent, as also evidenced by the modifications occurring to the coatings upon prolonged light exposure. Finally, the effect of light stabilizers on the weathering behavior of the LSC devices is also investigated.

The ultimate aim of this study is to achieve a greater understanding of structure-property relationships in crosslinked fluorinated coatings subjected to long-term light exposure and to provide useful guidelines for the design of high durability fluorescent coatings to be employed in the field of light management and photovoltaics.

2. Experimental

2.1. Materials

All materials employed in this study are of commercial source and were used as received. A perylene-based fluorescent dye (Lumogen F Red 305, BASF) was used as the fluorescent doping species in all polymeric coatings presented in this work. Its molecular structure and its absorption and emission spectra are presented in Fig. 1a and b, respectively. Poly(methyl methacrylate)–PMMA (Perspex XT, Lucite) was used as polymeric carrier in reference luminescent coatings. Lumiflon LF-910LM (Asahi Glass Company Ltd.), a chloro-trifluoro-ethylene-vinyl-ether (CTFEVE)-based polymer, was employed as fluorinated polymeric binder in all crosslinked coatings studied in this work. Three different crosslinked coating systems were obtained by selectively reacting this fluorinated binder with three different crosslinking agents, namely an aliphatic polyisocyanate based on hexamethylene diisocyanate (HDI) trimer (Tolonate HDT-LV2 by Perstorp) (from here on referred to as LT system), a cycloaliphatic polyisocyanate based on isophorone diisocyanate (IPDI) (Vestanat T1890/100 by Evonik Industries AG) (from here on referred to as LV system) and a hexamethoxy-methyl-melamine (HMMM)-based crosslinker (Cymel 303 by Cytec Industries Inc.) (from here on referred to as LC system). A summary of the materials employed in this work to prepare crosslinked fluorinated coatings is presented in Fig. 1c.

2.2. Instrumentation

UV–vis, fluorescence and FTIR spectroscopy were performed on solid state samples deposited onto glass/quartz/KBr/CaF_2 substrates by spin-coating (WS-400B-NPP Spin-Processor, Laurell Technologies Corp.) at 1200 RPM for 40 s in air. The coating thickness was measured by optical profilometry (Microfocus, UBM). UV–vis absorption spectra were recorded in air at room temperature in transmission mode by means of a Jasco V-570 UV-VIS-NIR Spectrophotometer. Fluorescence emission spectra were recorded in air at room temperature on a Jasco FP-6600 Spectrofluorometer. FTIR spectra were recorded in air at room temperature on a Nicolet 760-FTIR Spectrophotometer. Differential scanning calorimetry (DSC) was performed on solid state samples using a Mettler-Toledo DSC/823e instrument at a scan rate of 20 K/min in N_2 environment. Thermogravimetric analysis (TGA) was performed on solid state samples using a Q500 TGA system (TA Instruments) from ambient temperature to 600 °C at a scan rate of 20 °C/min in air. Static optical contact angle (OCA) measurements on the polymeric coatings were performed with an OCA 20 (DataPhysics) equipped with a CCD photo-camera and with a 500-μL Hamilton syringe to dispense liquid droplets. Measurements were taken at room temperature *via* the sessile drop technique. At least 20 measurements were performed in different regions on the surface of each coating and results were averaged. Water and diiodomethane were used as probe liquids. Atomic force microscopy (AFM) measurements were performed on the coatings by means of an Nscriptor DPNWriter (NanoInk) in tapping mode with a scan rate of 0.3 Hz using conventional Si tips (ACT probes by AppNano). All luminescent coatings were subjected to weathering tests under continuous Xenon light illumination in a weather-o-meter chamber (Solarbox 3000e, Cofomegra S.r.l.) equipped with an outdoor filter cutting all wavelengths below 280 nm. The total irradiance was measured by means of a power-meter with thermopile sensor (Ophir) and found to be approximately 1000 W m^{-2} (550 W m^{-2} in the 300–800 nm wavelength range [36]) for the entire duration of the test (>1000 h). The UV-light irradiance level in the 295–400 nm range was 50 W m^{-2}, as measured by means of a UV-photodiode. The relative humidity and the working temperature inside the

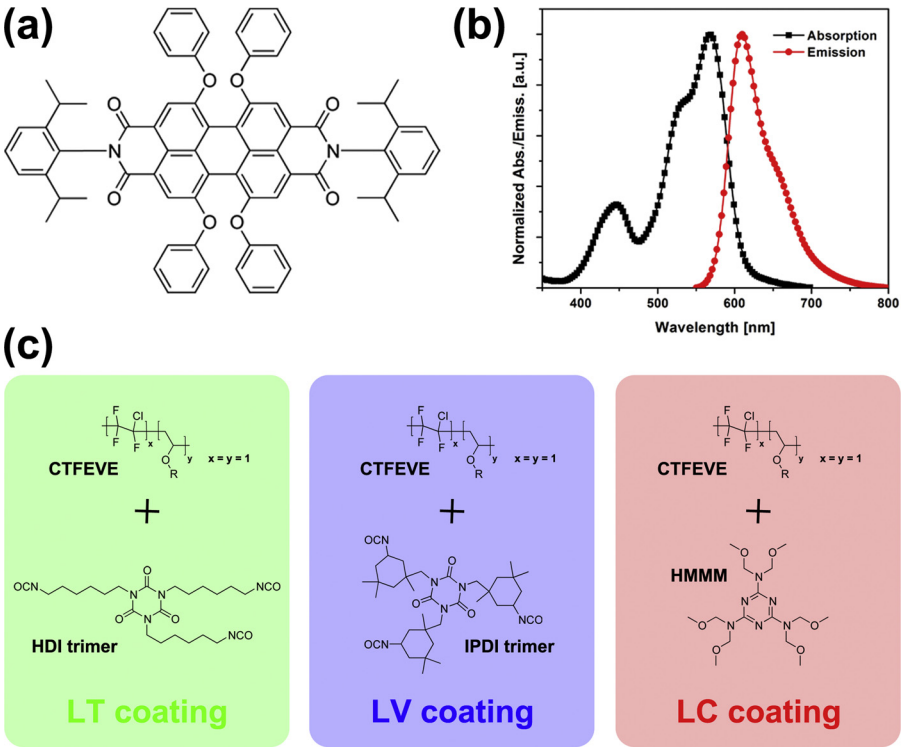

Fig. 1. (a) Molecular structure, (b) absorption/emission spectra of the fluorescent organic dye employed in this work, and (c) basic structural units of the materials employed in this work to prepare the new crosslinked fluorinated coatings: CTFEVE – chloro-trifluoro-ethylene-vinyl-ether (some of the R-groups are hydrogens, leading to the presence of reactive hydroxy groups – 100 mg KOH/g polymer), HDI – hexamethylene diisocyanate, IPDI – isophorone diisocyanate, HMMM – hexamethoxy-methyl-melamine.

testing chamber were maintained constant and measured to be 20% and 38 °C, respectively. The illuminated LSC/solar cell systems (from here on referred to as LSC devices) were characterized by recording current–voltage (*I–V*) curves by means of a Keithley 2612 source-measure unit under AM 1.5 G solar illumination at 1000 W m^{-2} (1 sun) (Abet Technologies 150 W solar simulator), calibrated with a NREL certified reference cell (PV Measurements). *I–V* testing was carried-out in air by performing scans between −0.2 V and 0.6 V with 10 mV steps on the illuminated LSC device and by recording the current response. The solar simulator power output was monitored by means of a power-meter with thermopile sensor (Ophir).

All normalized trends presented in this work for UV–vis absorption, fluorescence emission and device efficiency were calculated by dividing the value measured at a given exposure time by the value measured at 0 h of exposure.

2.3. Device fabrication

All LSC devices were fabricated on glass substrates (50 mm× 25 mm × 1 mm microscope slides, Thermo Scientific). For reference PMMA-based LSC systems, solid PMMA was dissolved in chloroform (15 wt% solution) under magnetic stirring, in the presence of the organic luminescent dye (5 wt%). For the preparation of LT- and LV-based systems, a 20 wt% chloroform solution of Lumiflon LF910-LM and Tolonate HDT-LV2 (for LT-coatings) or Lumiflon LF910-LM and Vestanat T1890/100 (for LV-coatings) was prepared under magnetic stirring (NCO/OH = 0.97), followed by the addition of the luminescent organic dye (4 wt%). For LC-based luminescent coatings, a 20 wt% chloroform solution of Lumiflon LF910-LM and Cymel 303 (80:20 w/w) was prepared under magnetic stirring, followed by the addition of the luminescent organic dye (4 wt%). In stabilized systems, 1 wt% of a NOR-HALS stabilizing agent (Tinuvin 123, CIBA) was also added to the stirring solution. Right before the spin-coating deposition process, a catalyst solution (di-*n*-butyltin dilaurate in chloroform for LT- and LV-systems, *p*-toluene sulfonic acid in ethanol for LC-systems) was added to each fluorinated system (0.1 wt% for LT- and LV-coatings, 1 wt% for LC-coatings). The fluorinated-polymer luminescent solution was then spin-cast onto the glass substrate in air (1200 RPM, 40 s) and allowed to crosslink in an oven at 150 °C for 30 min. After thermal annealing, complete crosslinking was achieved for all fluorinated systems, as evidenced by the resistance of the crosslinked coatings to solvent rubbing (MEK double rub test [37]). In addition, disappearance of the N=C=O stretching signal (2270 cm^{-1}) in the FTIR spectrum of the annealed LT- and LV-coatings was also observed, indicating complete reaction of all the NCO groups present in the polyisocyanates with the corresponding OH groups present in Lumiflon LF910-LM. The PMMA-based LSC coatings were instead dried out in air after the spin-casting process prior to further processing. The final coating thickness was found to be 6 μm, 6 μm, 5 μm and 9 μm for LT, LV, LC and PMMA coatings, respectively. The so-formed LSC coatings were then coupled to a mc-Si PV cell (SLSD-71N400 - active area 45.2 mm^2, average power conversion efficiency of 9.5%, by Silonex Inc.) so that one edge of the glass substrate was connected to the photoactive area of the PV cell. Bonding was performed by means of a hotmelt thermosoftening polyurethane adhesive (Krystalflex PE399, by Huntsman Polyurethanes) 0.5 mm thick that was placed on the active face of the PV cell after positioning the PV cell face-up on a 140 °C hot-plate. Once softening of the polyurethane film was achieved (approximately 2 min at 140 °C), one edge of the LSC glass substrate was pressed onto the adhesive film for about 30 s to ensure a good optical contact with the solar cell. The LSC system was then allowed to cool down to room temperature so that hardening of the polyurethane could be achieved. This ensured firm bonding between the solar cell and the LSC and good handling resistance.

3. Results and discussion

PMMA currently represents the material-of-choice as host matrix in standard LSC devices. However, its limited photostability as thin coating negatively affects the lifetime of PMMA-based LSC devices. Alternative polymeric systems that can ensure significantly improved outdoor stability of LSCs are therefore urgently needed. In this regard, the use of fluorinated polymer coatings for outdoor applications represent a way to achieve high weathering resistance and long-term durability in a variety of technological fields, due to the higher dissociation energy of the carbon-fluorine bond (105.4 kcal/mol) compared to the carbon-hydrogen bond (98.8 kcal/mol) [38] that imparts improved resistance to photodegradation. The main drawback in the use of fluoropolymer is their very limited compatibility and miscibility with common organic dyes. To this end, a particular class of fluorocarbon binders based on CTFEVE copolymers (Lumiflon LF-910LM, Fig. 1c) was employed in all fluorescent coatings herein considered. Because of the presence of both carbon-fluorine and carbon-chlorine bonds in its repeating unit, such fluoropolymer can guarantee sufficiently high polarity and good solubility in most organic solvents (including aromatics), and allow easy incorporation and dissolution of the luminescent organic dye used in this work. To further improve the environmental stability of the LSC coatings, this fluoropolymer was crosslinked with either an aliphatic polyisocyanate (based on either HDI or IPDI) to yield crosslinked coatings based on urethane bonds (LT- and LV-systems), or with a melamine-based crosslinker to yield a crosslinked coating based on ether-bonds (LC-system) (Fig. 1c). Indeed, a crosslinked coating can guarantee lower permeability toward oxygen and moisture compared to a non-crosslinked structure because of its lower free-volume. This is expected to yield a slower rate of photodegradation of the polymeric coating and thus a longer lifetime of the corresponding LSC devices.

Differential scanning calorimetry (DSC) was used to evaluate the glass transition temperature (T_g) of the crosslinked matrices. For LSC purposes, the T_g of the polymer coating should in principle be higher than room temperature in order to slow down degradation effects due to prolonged outdoor exposure to high temperatures. As presented in Table 1, a T_g value well above room temperature is found for all pristine dye-doped fluorinated systems (64 °C for LT, 108 °C for LV and 94 °C for LC), thus confirming their suitability to outdoor use. In particular, an almost two-fold increase in T_g value is observed when the CTFEVE-fluoropolymer is crosslinked with the IPDI-based polyisocyanate (LV coating) as compared to the HDI-based polyisocyanate (LT coating). Such an increase can be explained by taking into account the considerably higher T_g value of the IPDI-based crosslinker ($T_g \approx 73$ °C) compared to the HDI-based crosslinker ($T_g \approx -75$ °C).

In order to evaluate the physical response of the polymeric coatings to long-term weathering, DSC measurements were also performed after 1000 h of light exposure in a weather-o-meter chamber. As evident from Table 1, the crosslinked coatings do not appear to undergo significant changes upon long-term light exposure. In fact, only a minor decrease of T_g (approximately 3 °C lower) is found for these systems. On the contrary, the dye-doped PMMA-based coating shows a larger decrease in T_g after 1000 h of light exposure (from 116 °C to 108 °C), which may be attributed to a decrease in the polymer molecular weight resulting from photodegradation phenomena (depolymerization) occurring upon prolonged light exposure, or more probably to some plasticization effect [18].

The thermal stability of the fluorinated coatings was also investigated through TGA analysis (Supporting Information). All systems showed decomposition temperatures at 5% weight loss above 200 °C, likely ascribable to cleavage of the crosslinking bonds. This thermal behavior indicates that for all crosslinked coatings the presence of the fluorinated units allows to achieve satisfactory thermal stability for the target application.

The wettability of the surface of all the fluorescent coatings was investigated by means of static contact angle measurements with water and diiodomethane, and the surface tension γ of each system including its dispersive and polar components (γ^d and γ^p, respectively) was calculated using the Wu method [39]. The results are shown in Table 2. All pristine fluorinated coatings present a moderate hydrophobic character with water contact angles θ_{H_2O} of 94.4°, 92.8° and 93.4° for LT, LV and LC systems, respectively. In addition, similar surface tension values are found for all fluorinated coatings (35.4 mN/m, 35.3 mN/m, and 34.6 mN/m for LT, LV and LC, respectively), indicating that the type of crosslinking network (urethane bonds for LT and LV, ether bonds for LC) does not significantly influence the surface behavior of the coatings. On the contrary, hydrophobicity is lower with PMMA ($\theta_{H_2O} = 69.5°$), which also shows the highest surface tension value ($\gamma = 48.5$ mN/m). It is worth underlying that all crosslinked coatings show values of the polar component of the surface tension γ^p (5–6 mN/m) higher than what found in other fluorinated systems, where this contribution usually plays a minor role. This behavior can be attributed to the presence of C—Cl bonds in the CTFEVE binder chain that increase the polarity of the coating [40–42]. After 1000 h of light exposure, only small modifications on the wettability behavior of the coatings are observed, indicating that the surface energy of the systems is not substantially affected by weathering.

The surface morphology of the fluorescent coatings was investigated by means of atomic force microscopy (AFM) on pristine and weathered systems. As shown in Fig. 2, where AFM topography images of all coatings are presented, the nanoscale morphology of the pristine fluorinated systems appears slightly coarser compared to PMMA-based coatings. In particular, large surface features such as bumps and valleys are observed in the LC system (LC – 0 h), gradually decreasing in size in LV (LV – 0 h) and LT (LT – 0 h) films. In accordance with these observations, the surface root-mean-square roughness R_{RMS} of LC coatings is found to be the highest ($R_{RMS} = 1.94$ nm) among the fluorinated systems, followed by LV ($R_{RMS} = 0.62$ nm) and LT ($R_{RMS} = 0.52$ nm). As opposed to this, PMMA coatings show a very smooth surface with an R_{RMS} value as low as 0.23 nm.

After prolonged light exposure (1000 h), coarsening of the surface morphology is observed on all coating systems, resulting in a general increase in surface roughness. In particular, an R_{RMS} value as high as 3.06 nm is found in weathered LC systems (LC – 1000 h), as opposed to 1.05 nm and 0.67 nm for LV (LV – 1000 h) and LT (LT – 1000 h), respectively. A slightly smoother surface is again observed on weathered PMMA coatings (PMMA – 1000 h) with an R_{RMS} of 0.42 nm, which represents however a two-fold R_{RMS} increase compared to the pristine PMMA coating.

The UV–vis absorption spectrum of the fluorescent organic dye molecule used in all LSC coatings is characterized by two different absorption peaks, as presented in Fig. 1b. It has been shown in a previous work [16] that the shorter-wavelength absorption peak can be attributed to the absorption of the four phenoxy groups in *bay*-positions in the dye molecule, while the higher-intensity longer-wavelength absorption peak is associated to the absorption of its perylene core. Fig. 3a presents the evolution of the absorption intensity of such perylene-core absorption peak upon increasing light exposure time for all polymeric systems investigated in this work. A decrease of absorption intensity at increasing light exposure time is observed in all systems, even though some differences can be highlighted. In particular, the LC coating manifests an over 60% absorption intensity decay after 1000 h of light exposure, which is much higher compared to the other fluorinated crosslinked matrices that only lose 35% (LT) and 20% (LV) of their initial absorption intensity. A similar trend is observed for PMMA,

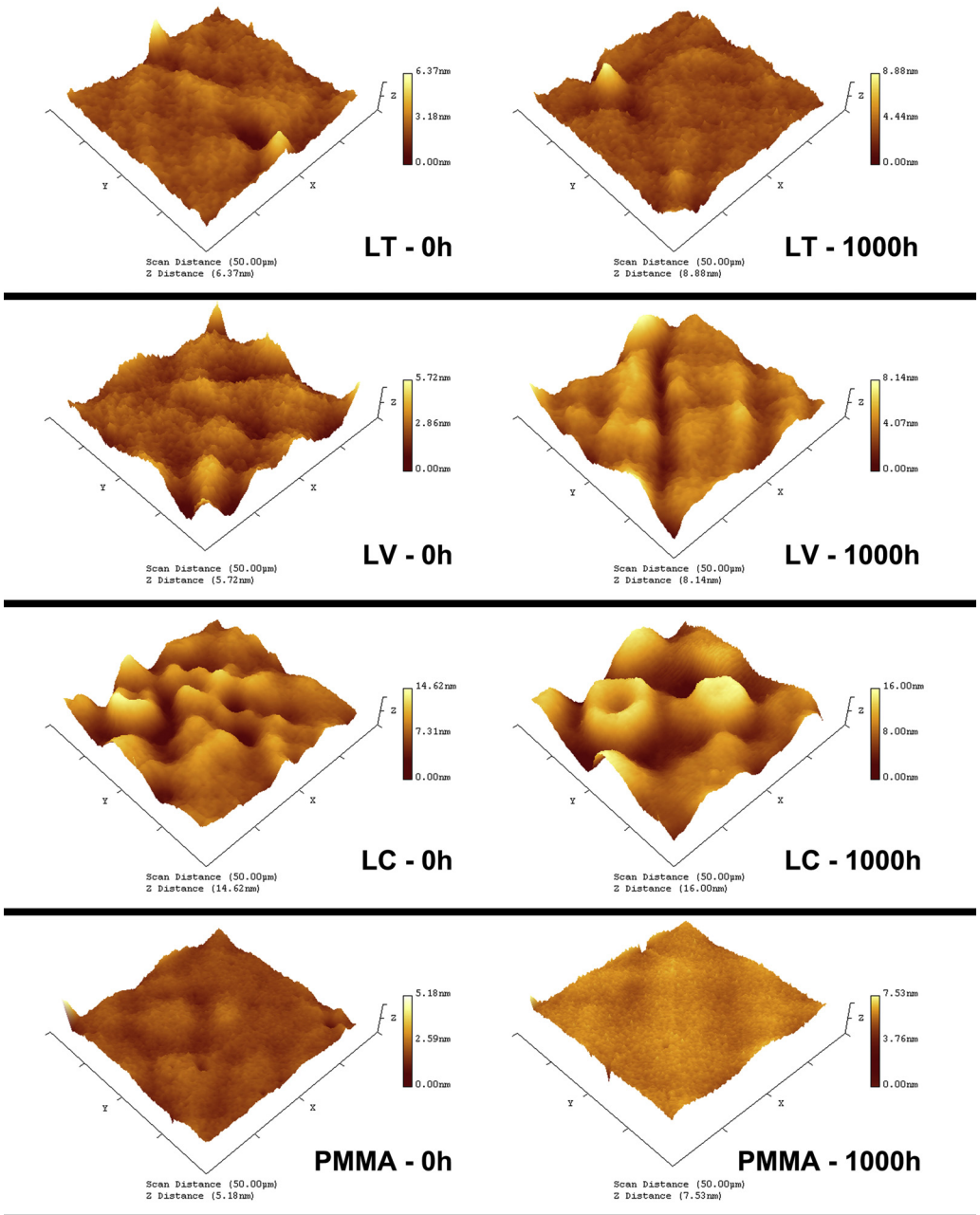

Fig. 2. AFM topography 3D images (50 µm × 50 µm) of LT, LV, LC and PMMA fluorescent coatings before (0 h) and after (1000 h) long-term light exposure in a weather-o-meter chamber.

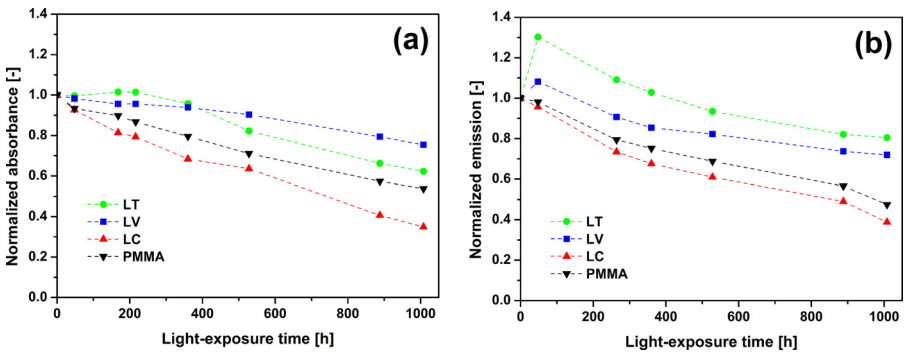

Fig. 3. Normalized (a) absorption intensity and (b) fluorescence emission intensity of LT, LV, LC and PMMA fluorescent coatings over light-exposure time in a weather-o-meter chamber (each trend was normalized with respect to the corresponding value measured at 0 h).

Table 1
Glass transition temperature T_g for all dye-doped coatings investigated in this work, measured by means of DSC analysis on pristine (t_w = 0 h) and weathered (t_w = 1000 h) systems.

	LT system	LV system	LC system	PMMA system
T_g (t_w = 0 h)	64 °C	108 °C	94 °C	116 °C
T_g (t_w = 1000 h)	60 °C	106 °C	91 °C	108 °C

Table 2
Static contact angles (θ_{H_2O}, $\theta_{CH_2I_2}$), total surface tension (γ) and its dispersive (γ^d) and polar (γ^p) components for LT, LV, LC and PMMA coatings, before (t_w = 0 h) and after (t_w = 1000 h) prolonged light exposure.

	θ_{H_2O} (t_w = 0 h) [°]	θ_{H_2O} (t_w = 1000 h) [°]	$\theta_{CH_2I_2}$ (t_w = 0 h) [°]	$\theta_{CH_2I_2}$ (t_w = 1000 h) [°]	Surface tension (t_w = 0 h) [mN/m]	Surface tension (t_w = 1000 h) [mN/m]
LT	94.4 ± 0.8	93.2 ± 2.6	51.9 ± 0.6	53.8 ± 1.4	35.4 ± 0.5 (γ) 30.3 ± 0.3 (γ^d) 5.1 ± 0.3 (γ^p)	34.9 ± 1.3 (γ) 29.3 ± 0.7 (γ^d) 5.7 ± 1.1 (γ^p)
LV	92.8 ± 0.7	92.5 ± 2.2	53.4 ± 0.6	53.8 ± 0.5	35.3 ± 0.4 (γ) 29.4 ± 0.3 (γ^d) 5.9 ± 0.3 (γ^p)	35.2 ± 0.9 (γ) 29.2 ± 0.3 (γ^d) 6.1 ± 0.9 (γ^p)
LC	93.4 ± 0.8	92.1 ± 1.8	54.7 ± 0.7	55.7 ± 0.4	34.6 ± 0.5 (γ) 28.8 ± 0.4 (γ^d) 5.8 ± 0.3 (γ^p)	34.6 ± 0.8 (γ) 28.3 ± 0.3 (γ^d) 6.4 ± 0.8 (γ^p)
PMMA	69.5 ± 1.6	72.4 ± 1.1	42.7 ± 1.3	43.5 ± 0.8	48.5 ± 0.9 (γ) 33.0 ± 0.6 (γ^d) 15.5 ± 0.8 (γ^p)	46.8 ± 0.6 (γ) 32.7 ± 0.4 (γ^d) 14.1 ± 0.5 (γ^p)

whose absorption intensity after 1000 h of light exposure is 45% lower compared to its initial value.

The emission spectrum of the fluorescent dye is shown in Fig. 1b and is characterized by a sharp single emission peak attributed to the fluorescence of the perylene core in the dye molecule. As presented in Fig. 3b, the emission intensity in LC and PMMA fluorescent coatings undergoes a constant decrease upon light exposure, leading to an approximately 50% drop after 1000 h. As opposed to that, the other crosslinked fluorinated systems (LT and LV coatings) only show a ~20% emission intensity drop after long-term light exposure. In addition, an increase of emission intensity in the first 100 h of light exposure is found in LT and LV systems, which appears to be clearly dependent on the chemical environment surrounding the fluorescent dye molecule as only coatings based on urethane linkages (LT and LV) show this effect. This behavior may be ascribed to the morphological rearrangement of the organic dye molecules within the polymeric host matrix following light irradiation, which may lead to improved dye solubility in the specific polymeric system and therefore enhance the fluorescence emission (organic dye dimers and aggregates are non-fluorescent [43,44]). It is likely that good dye solubility is already achieved in LC and PMMA coatings, where this effect is not evident [28].

The FTIR spectra of the fluorescent systems were collected in the attempt to highlight chemical modifications occurring to the coatings upon light exposure (FTIR spectra of reactants are included in the Supporting Information). Fig. 4 presents the FTIR spectra of LT, LV, LC and PMMA fluorescent systems before and after 500 h and 1000 h of light exposure. As evidenced by the FTIR spectra of pristine LT and LV systems, the N=C=O stretching signal (2270 cm^{-1}) cannot be detected, further confirming that the reaction between all the NCO groups in the polyisocyanate crosslinker and the corresponding OH groups present in the fluorinated polymer has completely occurred. When subjected to prolonged light exposure, LT and LV fluorescent systems does not appear to undergo significant modifications as no new signals in the FTIR spectra ascribable to the formation of new chemical groups or degraded species can be observed (Fig. 4a and b). These results may indicate that fluorinated coatings crosslinked *via* a urethane-based network are sufficiently stable to photodegradation and may represent good candidates for use in durable LSC devices. Conversely, some changes can be observed in LC and PMMA fluorescent coatings upon light exposure.

In particular, both systems are characterized by the appearance of FTIR absorption signals due to the stretching of OH groups in the 3600–3400 cm^{-1} region upon light exposure, likely due to the formation of degraded oxidized species. Furthermore, the emergence of an absorption signal at 1720 cm^{-1} (C=O stretching vibration) in LC coatings, whose intensity progressively increases with light exposure time, may indicate the formation of carbonyl species resulting from photodegradation of the polymer (Fig. 4c). Similarly, the appearance of two broad bands in the carbonyl region adjacent to the main peak centered at 1730 cm^{-1} in PMMA coatings (Fig. 4d) indicates photooxidation of the polymeric matrix [18,45]. Finally, an overall decrease of the absorption intensity is observed in the entire FTIR spectrum of both LC and PMMA after prolonged light exposure, as opposed to LT and LV systems where no significant intensity changes are found. These results suggest that the poorer stability of LC and PMMA coatings may lead to shorter LSC device lifetime, as the degradation of the polymer may cause progressively more frequent trapping of the emitted photons within the polymeric host matrix, thus resulting in a decrease of the photon transport efficiency within the LSC.

To correlate the effects of the modifications occurring to the polymeric materials discussed so far with device lifetime, all fluorescent coatings were employed to fabricate thin-film LSC devices that were subjected to continuous illumination (no dark cycles) in a weather-o-meter chamber for over 1000 h. PV tests under simulated sunlight were periodically conducted on all LSC devices to evaluate their operational stability over time.

To evaluate the PV response of LSC devices, the absolute power conversion efficiency η_{abs} of each LSC was calculated, defined as follows:

$$\eta_{abs} = FF\frac{(I_{SC}/A^{(LSC)})V_{OC}}{P_{IN}} \quad (1)$$

with FF [–], I_{SC} [mA], V_{OC} [V], $A^{(LSC)}$ [cm^2] being the fill factor, the short-circuit current, the open-circuit voltage and the front area of the LSC device, respectively and P_{IN} the incident solar power

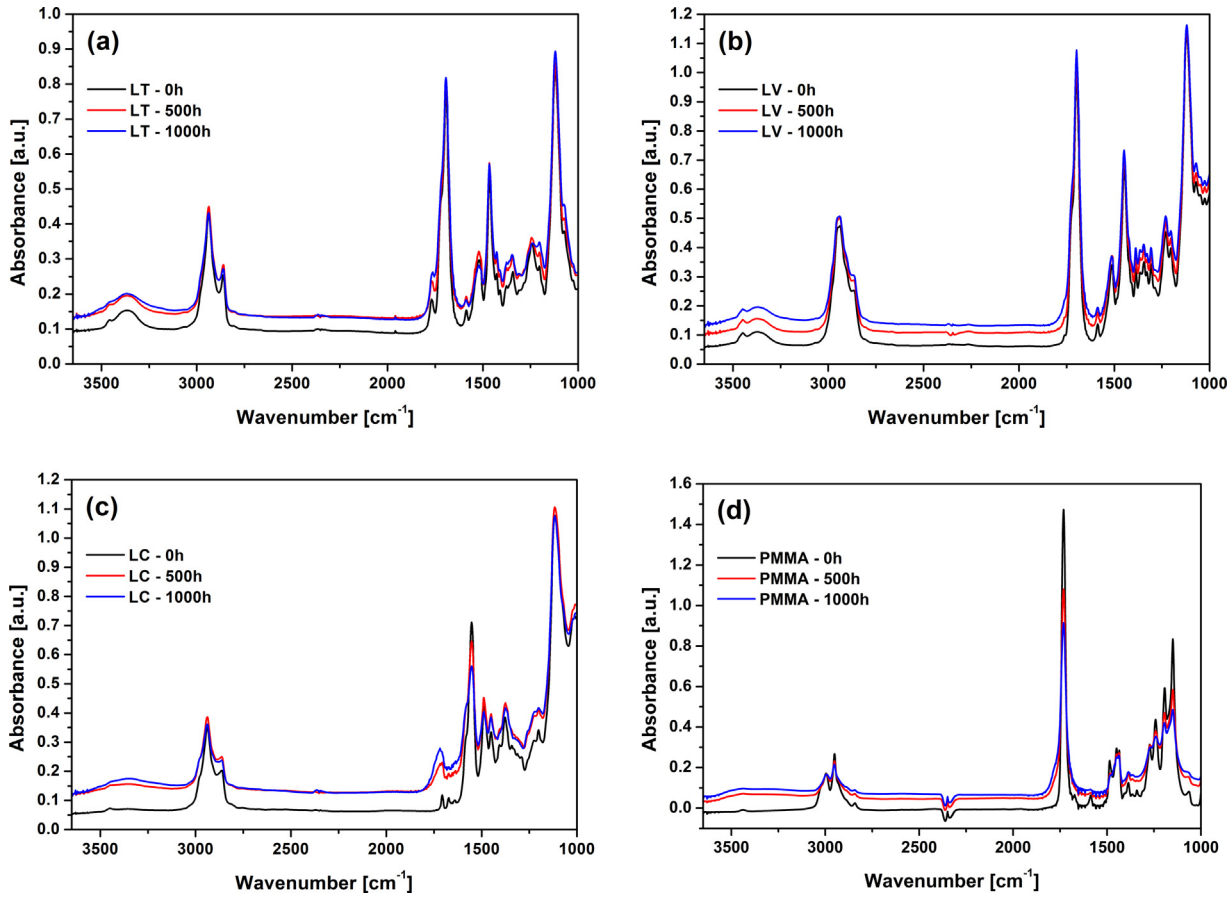

Fig. 4. FTIR absorption spectra of (a) LT, (b) LV, (c) LC, and (d) PMMA fluorescent coatings before (0 h) and after 500 h and 1000 h of light-exposure in a weather-o-meter chamber.

density [mW cm^{-2}]. In order to obtain a measure of the variation of the performance of the PV cell after coupling it to a thin film LSC, the power conversion efficiency gain $\Delta\eta$ was also calculated as follows:

$$\Delta\eta = \frac{\eta_{rel} - \eta_{PV}}{\eta_{PV}} \quad (2)$$

with η_{PV} being the power conversion efficiency of the bare PV cell under direct illumination and η_{rel} being defined as follows ($A^{(PV)}$ is the active area of the PV cell):

$$\eta_{rel} = FF\frac{(I_{SC}/A^{(PV)})V_{OC}}{P_{IN}} \quad (3)$$

Positive values of $\Delta\eta$ indicate that the use of an LSC device (PV cell coupled to a thin-film LSC) yields an actual gain in power conversion efficiency with respect to the bare PV cell.

In order to verify the suitability of the new fluorinated crosslinked coatings to serve as luminescent thin films for LSC device applications, the PV response of all pristine systems was first evaluated and compared to reference PMMA-based devices. All new fluorinated LSC systems were found to achieve similar PV performance, with η_{abs} = 0.49% ($\Delta\eta$ = 27%), η_{abs} = 0.47% ($\Delta\eta$ = 33%) and η_{abs} = 0.51% ($\Delta\eta$ = 36%) for LT, LV and LC pristine devices, respectively. On the other hand, PMMA-based systems yielded efficiencies of 0.51% (η_{abs}) and 41% ($\Delta\eta$). These results indicate that all new fluorinated crosslinked LSC systems are able to guarantee starting efficiency values not far from those obtained with reference PMMA-based devices. The slightly higher efficiencies reported for PMMA-based devices may be ascribed to better chemical affinity and solubility of the organic dye in PMMA than in the fluorinated matrices, as evidenced previously [28], since it is known that dye aggregates or dimers are not fluorescent [43,44].

Fig. 5 presents the PV behavior of all fluorinated LSC devices upon continuous long-term light exposure (no dark cycles). For benchmarking purposes, also PMMA-based devices have been included. After 1000 h of light exposure PMMA-based devices undergo a significant decrease of performance, with a η_{abs} drop of almost 30% (Fig. 5a), accompanied by a nearly 80% decrease of $\Delta\eta$ (Fig. 5b). Similar trends are observed in LC devices, where an 80% $\Delta\eta$ drop is observed after 1000 h of continuous light exposure (Fig. 5b). On the other hand, both urethane-based crosslinked systems (LT and LV) show very different behaviors. In both systems, an efficiency increase is found in the first 100 h of weathering, which can be correlated with the changes observed in the fluorescence emission spectra discussed earlier (Fig. 3b). In addition, only a 5% η_{abs} drop is reported upon long-term irradiation, while $\Delta\eta$ is found to decrease of about 30%. These results are consistent with the trends observed in the UV–vis and FTIR spectra presented earlier (Fig. 3a, Fig. 4), and represent a further confirmation of the critical role played by the polymeric system in the operational stability of thin-film LSC devices. Similar trends were also found in aging experiment on the same LSC devices under UV-A light (Supporting Information). The differences observed between LC and LT/LV devices in the long-term light exposure regime may be correlated with the different chemical nature of crosslinking bonds present in each crosslinked matrix. While for LT and LV systems a urethane-bond network is formed upon crosslinking, LC coatings undergo crosslinking through the formation of ether bonds. The latter appear to be more prone to photodegradation, thus yielding a constant decrease of device performance upon continuous light

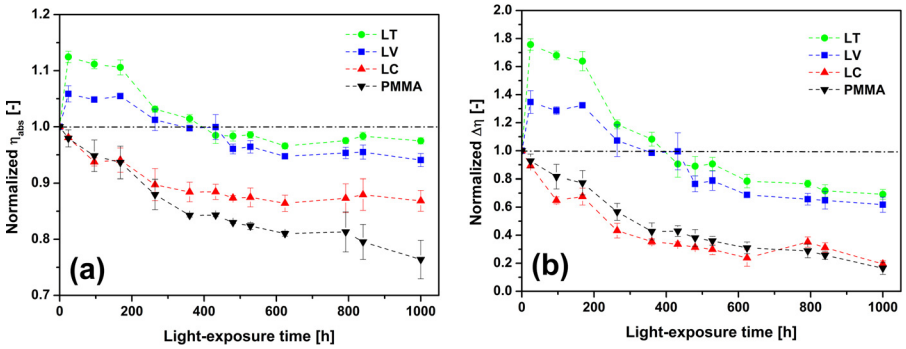

Fig. 5. Normalized trends of (a) absolute power conversion efficiency η_{abs} and (b) power conversion efficiency gain $\Delta\eta$ at increasing exposure time for LT, LV, LC and PMMA-based LSC devices (each trend was normalized with respect to the corresponding value measured at 0 h).

exposure. As a result, fluorinated polyurethane-based crosslinked coatings seem to be the most promising alternative to PMMA for long-term stability of LSC device performance.

In many applications, polymeric coatings employed for high outdoor durability are typically doped with additives to increase their stability toward sunlight. Hindered amine light stabilizers (HALS) or partially oxidized NOR-HALS [45] are an example of this class of additives, as they are normally employed as radical scavengers to slow down the rate of photooxidative degradation of polymeric systems. Accordingly, NOR-HALS radical scavengers were employed in all LSC systems investigated in this work in order to potentially increase further the lifetime of the corresponding devices. The addition of stabilizing additives was not shown to significantly affect the PV response of pristine LSC devices, as all stabilized systems yielded efficiencies comparable to those found on virgin coatings (η_{abs} = 0.48%, 0.49%, 0.50% and 0.53% for LT-NH, LV-NH, LC-NH and PMMA-NH, respectively).

Fig. 6 presents the η_{abs} trends as a function of light exposure time for all stabilized systems investigated in this work, together with the corresponding undoped systems. For all fluorinated LSCs, large differences between virgin and stabilized devices are observed in the first part of the weathering tests (<200 h), where the stabilized devices undergo a sharper η_{abs} decrease compared to virgin systems. However, for longer light exposure times (>300 h) this tendency is partially reversed as the PV performance of doped systems appears to stabilize over time. In particular, LT-NH and LV-NH systems show efficiency trends comparable with the corresponding non-stabilized counterparts for long light exposure times (>800 h) (Fig. 6a and b). Furthermore, in LC-NH and PMMA-NH devices, this long-term stabilizing effect is even more pronounced as the PV response in these systems seems to improve over time and ultimately exceed the corresponding undoped systems (Fig. 6c and d). Such delayed stabilizing effect may be explained by considering the induction time needed for the activation of the stabilizing additive molecule, which might be in the order of a few hundred hours in all systems.

In conclusion, the PV trends reported on stabilized LSC devices suggest that NOR-HALS may act as effective stabilizing agents for all coating systems considered in this work, especially in the long-term light exposure regime (>600 h).

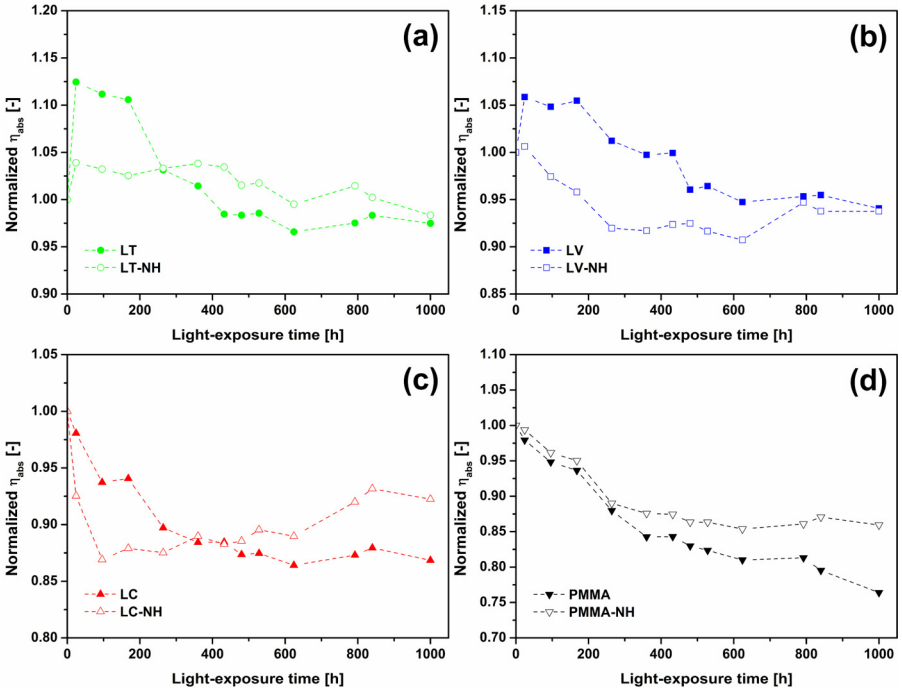

Fig. 6. Normalized trends of absolute power conversion efficiency η_{abs} at increasing light exposure time for (a) LT and stabilized LT-NH devices, (b) LV and stabilized LV-NH devices, (c) LC and stabilized LC-NH devices, and (d) PMMA and stabilized PMMA-NH devices (each trend was normalized with respect to the corresponding value measured at 0 h).

4. Conclusions

New crosslinked fluoropolymer coatings were presented in this work as novel fluorescent materials for thin film LSC devices. The new polymeric systems were obtained by crosslinking a functional CTFEVE-copolymer with three different curing agents, namely an aliphatic polyisocyanate based on HDI, a cycloaliphatic polyisocyanurate based on IPDI and a melamine-based crosslinker. All the new coatings were subjected to continuous illumination in a weather-o-meter chamber for over 1000 h and a full characterization of the new coatings upon light exposure was carried out. In the attempt to correlate the chemical, physical and morphological modifications occurring to the fluorescent coatings with LSC device stability, all the new coatings were employed to fabricate functioning LSC devices that were also tested against long term light exposure. As opposed to melamine-based and control PMMA-based devices that exhibited a sharp decrease in PV efficiency for increasing light exposure time, polyurethane-based devices were able to retain more than 90% of their initial device efficiency η_{abs} even after 1000 h of light exposure. These trends were shown to correlate well with the chemical modifications observed on the same coatings. In addition, the effect of radical scavenging additives on LSC device operational stability was investigated and it was found that in the long-term light exposure regime (>600 h) these additives may lead to improvements in LSC device lifetime.

The results of this study demonstrate that the use of fluorescent crosslinked fluorinated systems as alternative to PMMA represents a very promising approach to achieve high durability coatings to be employed in LSC and light management applications.

Acknowledgements

The authors gratefully acknowledge Dr. Luigi Brambilla, Dr. Mirella Del Zoppo and Prof. Chiara Castiglioni for helpful discussions.

Appendix A. Supplementary data

Supplementary data associated with this article can be found, in the online version.

References

[1] M.G. Debije, P.P.C. Verbunt, Adv. Energy Mater. 2 (2012) 12–35.
[2] M.J. Currie, J.K. Mapel, T.D. Heidel, S. Goffri, M.A. Baldo, Science 321 (2008) 226–228.
[3] G. Smestad, H. Ries, R. Winston, E. Yablonovitch, Sol. Energy Mater. 21 (1990) 99–111.
[4] D.J. Farrell, M. Yoshida, Prog. Photovolt: Res. Appl. 20 (2011) 93–99.
[5] H. Hernandez-Noyola, D.H. Potterveld, R.J. Holt, S.B. Darling, Energy Environ. Sci. 5 (2012) 5798–5802.
[6] G. Kocher-Oberlehner, M. Bardosova, M. Pemble, B.S. Richards, Sol. Energy Mater. Sol. Cells 104 (2012) 53–57.
[7] J.W.E. Wiegman, E. van der Kolk, Sol. Energy Mater. Sol. Cells 103 (2012) 41–47.
[8] C. Corrado, S.W. Leow, M. Osborn, E. Chan, B. Balaban, S.A. Carter, Sol. Energy Mater. Sol. Cells 111 (2013) 74–81.
[9] R. Bose, D.J. Farrell, A.J. Chatten, M. Pravettoni, A. Buchtemann, K.W.J. Barnham, Proc. of 22nd European Photovoltaic Solar Energy Conference (22nd EUPVSEC), Milan, Italy, 2007, pp. 210–214.
[10] G. Seybold, G. Wagenblast, Dyes Pigments 11 (1989) 303–317.
[11] O.A. Bozdemir, S. Erbas-Cakmak, O.O. Ekiz, A. Dana, E.U. Akkaya, Angew. Chem. Int. Ed. 50 (2011) 10907–10912.
[12] G. Katsagounos, E. Stathatos, N.B. Arabatzis, A.D. Keramidas, P. Lianos, J. Lumin. 131 (2011) 1776–1781.
[13] R. Reisfeld, Opt. Mater. 32 (2010) 850–856.
[14] J. Bomm, A. Buchtemann, A.J. Chatten, R. Bose, D.J. Farrell, N.L.A. Chan, Y. Xiao, L.H. Slooff, T. Meyer, A. Meyer, W.G.J.H. van Sark, R. Koole, Sol. Energy Mater. Sol. Cells 95 (2011) 2087–2094.
[15] N. Tanaka, N. Barashkov, J. Heath, W.N. Sisk, Appl. Opt. 45 (2006) 3846–3851.
[16] G. Griffini, L. Brambilla, M. Levi, M. Del Zoppo, S. Turri, Sol. Energy Mater. Sol. Cells 111 (2013) 41–48.
[17] W.G.J.H. van Sark, K.W.J. Barnham, L.H. Slooff, A.J. Chatten, A. Buchtemann, A. Meyer, S.J. McCormack, R. Koole, D.J. Farrell, R. Bose, E.E. Bende, A.R. Burgers, T. Budel, J. Quilitz, M. Kennedy, T. Meyer, C.D.M. Donega, A. Meijerink, D. Vanmaekelbergh, Opt. Express 16 (2008) 21773–21792.
[18] H. Kaczmarek, A. Kaminska, A. van Herk, Eur. Polym. J. 36 (2000) 767–777.
[19] B. Ranby, J.F. Rabek, Photodegradation, Photo-oxidation and Photostabilization of Polymers: Principles and Applications, John Wiley & Sons Ltd, 1975.
[20] A. Torikai, Wavelength selectivity of photodegradation of polymers, in: S.H. Hamid (Ed.), Handbook of Polymer Degradation, Marcel Dekker Inc, New York, 2000, pp. 573–603.
[21] R. Soti, E. Farkas, M. Hilbert, Z. Farkas, I. Ketskemety, J. Lumin. 68 (1996) 105–114.
[22] J.C. Goldschmidt, M. Peters, M. Hermle, S.W. Glunz, J. Appl. Phys. 105 (2009).
[23] I. Baumberg, O. Berezin, A. Drabkin, B. Gorelik, L. Kogan, M. Voskobojnik, M. Zaidman, Polym. Degrad. Stab. 73 (2001) 403–410.
[24] S.M. El Bashir, J. Lumin. 132 (2012) 1786–1791.
[25] Y.S. Lim, C.K. Lo, G.B. Teh, Renew. Energy 45 (2012) 156–162.
[26] M. Buffa, S. Carturan, M.G. Debije, A. Quaranta, G. Maggioni, Sol. Energy Mater. Sol. Cells 103 (2012) 114–118.
[27] V. Fattori, M. Melucci, L. Ferrante, M. Zambianchi, I. Manet, W. Oberhauser, G. Giambastiani, M. Frediani, G. Giachi, N. Camaioni, Energy Environ. Sci. 4 (2011) 2849–2853.
[28] G. Griffini, M. Levi, S. Turri, Sol. Energy Mater. Sol. Cells 118 (2013) 36–42.
[29] J. Scheirs, Modern Fluoropolymers High Performance Polymers for Diverse Applications, John Wiley & Sons Ltd, Chichester, 1997.
[30] D.M. Lemal, J. Org. Chem. 69 (2004) 1–11.
[31] R. Canteri, G. Speranza, M. Anderle, S. Turri, S. Radice, Surf. Interface Anal. 35 (2003) 318–326.
[32] S. Turri, M. Scicchitano, G. Simeone, C. Tonelli, Prog. Org. Coat. 32 (1997) 205–213.
[33] A. Alaaeddine, F. Boschet, B. Ameduri, B. Boutevin, J. Polym. Sci. Part A: Polym. Chem. 50 (2012) 3303–3312.
[34] G. Couture, B. Campagne, A. Alaaeddine, B. Ameduri, Polym. Chem. 4 (2013) 1960–1968.
[35] G. Tillet, P. De Leonardis, A. Alaaeddine, M. Umeda, S. Mori, N. Shibata, S.M. Aly, D. Fortin, P.D. Harvey, B. Ameduri, Macromol. Chem. Phys. 213 (2012) 1559–1568.
[36] Paints and varnishes – artificial weathering and exposure to artificial radiation – exposure to filtered xenon-arc radiation, second ed., ISO 11341:2004(E), 2004.
[37] Standard Practice for Assessing the Solvent Resistance of Organic Coatings Using Solvent Rubs, ASTM D5402-93, 1999.
[38] D. O'Hagan, Chem. Soc. Rev. 37 (2008) 308–319.
[39] S. Wu, J. Colloid Interface Sci. 71 (1979) 605–609.
[40] P. Fabbri, M. Messori, M. Montecchi, S. Nannarone, L. Pasquali, F. Pilati, C. Tonelli, M. Toselli, Polymer 47 (2006) 1055–1062.
[41] B. Ameduri, R. Bongiovanni, V. Lombardi, A. Pollicino, A. Priola, A. Recca, J. Polym. Sci. Part A: Polym. Chem. 39 (2001) 4227–4235.
[42] F. Montefusco, R. Bongiovanni, A. Priola, B. Ameduri, Macromolecules 37 (2004) 9804–9813.
[43] R.O. Al Kaysi, T.S. Ahn, A.M. Muller, C.J. Bardeen, Phys. Chem. Chem. Phys. 8 (2006) 3453–3459.
[44] K.A. Colby, J.J. Burdett, R.F. Frisbee, L. Zhu, R.J. Dillon, C.J. Bardeen, J. Phys. Chem. A 114 (2010) 3471–3482.
[45] F. Gugumus, Light stabilizers, in: H. Zweifel (Ed.), Plastics Additives Handbook, Carl Hanser Verlag, Munich, 2001, pp. 141–425.